Available online at www.sciencedirect.com
SCIENCE DIRECT®
Physica E 26 (2005) 245–251
PHYSICA E
www.elsevier.com/locate/physe

Strain interactions and defect formation in stacked InGaAs quantum dot and dot-in-well structures

M. Gutiérrez[a,*], M. Hopkinson[a], H.Y. Liu[a], J.S. Ng[a], M. Herrera[b], D. González[b], R. Garcia[b], R. Beanland[c]

[a]*Department of Electronic & Electrical Engineering, University of Sheffield, Mappin Street, Sheffield S1 3JD, UK*
[b]*Departamento de Ciencia de los Materiales e I.M y Q.I, Universidad de Cádiz, 11510 Puerto Real, Spain*
[c]*Bookham Technology PLC, Caswell, Towcester, Northamptonshire NN12 8EQ, UK*

Available online 2 December 2004

Abstract

The growth of high-quality stacked quantum dot (QD) structures represents one of the key challenges for future device applications. Electronic coupling between QDs requires closely separated electronic levels and thin barrier layers, requiring near identical composition and shape, despite strong strain interactions. This paper presents a detailed characterization study of stacked InGaAs QD and InAs/InGaAs dot-in-well (DWELL) structures using cross-sectional transmission electron microscopy. For $In_{.5}Ga_{.5}As$/GaAs QD structures we have observed optimized stacking using a barrier thickness ~12 nm.

We also report studies of stacking in DWELL laser structures. Despite reports of very low threshold currents in such lasers, designed for 1.3 μm emission, performance is limited by gain saturation and thermal excitation effects. We have explored solutions to these problems by stacking multiple DWELL layers of three, five and 10 repeats. Initial attempts at stacked multilayer structures, particularly samples with a large number of repeats, produced variable results, with a number of the final devices characterized by poor emission and electrical characteristics. Analysis by transmission electron microscopy has identified the presence of large defective regions arising from the complex interaction of dots on several planes and propagating threading dislocations into the cladding layers. The origin of this defect is identified as the coalescence of QDs at very high density and the resulting dislocation propagating to higher dot planes. An effective modified method to reduce the defect density by growing the barrier layer at higher temperature will be discussed. Finally, we report the growth of a stacked 10-layer structure using relatively thin barriers, grown using this technique.

PACS: 68.37.Lp; 68.65.Hb; 78.67.Hc

Keywords: Quantum dots; TEM; Stacking; Defects; Lasers

*Corresponding author. Tel.: +44 (0) 114-222-5163; fax: +44 (0) 114-272-6391.
E-mail address: m.gutierrez@shef.ac.uk (M. Gutiérrez).

1386-9477/$ - see front matter © 2004 Elsevier B.V. All rights reserved.
doi:10.1016/j.physe.2004.08.098

1. Introduction

InAs-based quantum dot (QD) lasers, using GaAs substrates, are the subject of considerable research effort due to their potential for application within the 1300–1550 nm fibre optical communication waveband. The InAs QD lasers offer potential improved performance in terms of low threshold current density and improved thermal stability, whilst exploiting lower cost GaAs technology. At present, such devices offer the potential prospect of displacing current InP-based technology for metropolitan (<10 km) links utilising the 1310 nm waveband. Although the use of nitrogen-containing devices on GaAs substrates has also been demonstrated as an alternative to InP-based devices, several approaches to this are being pursued in a number of laboratories. By far, the most successful to these employs the dot-in-well (DWELL) structure [1–4]. In the DWELL structure the InAs QDs are positioned within an $In_xGa_{1-x}As$ quantum well (QW) of low indium composition (x) of typically 0.1–0.2. The lowering of the emission energy in such structures is principally due to the reduction of the hydrostatic deformation on the strained QD. However, the structure of the QDs is also likely to be modified by a suppression of diffusion and/or segregation effects. One limitation of this method is the increased stress concentration around the dots, which acts as a possible source of dislocations.

1.3 μm GaAs/InAs QD lasers with ultra-low threshold current densities of $<50\,A\,cm^{-2}$ have now been routinely demonstrated [1,2]. In terms of temperature stability, values of the characteristic temperature (T_o), for 1.3 μm QD lasers, as high as 80 K, but more typically 30–50 K have been reported [3]. These values are generally lower than those achieved by current InP technology (90–110 K) and effort is needed to address this issue. The main limitations are carrier escape from the QD ground state and the relatively low gain per dot layer, leading to gain saturation. Whilst improved confinement layers may offer a solution to the first issue, the use of high in-plane dot densities and multiple layer stacking is the only effective method to reduce gain saturation [4]. This paper explores the multiple stacking of InAs DWELL structures.

We have found that dislocated QDs are often present even in isolated DWELL structures. Further defects occur due to the coalescence of DWELLs at the high densities used in our work. In multilayer structures, defects resulting from the two mechanisms can propagate to adjacent layers and relax large numbers of overlying QDs.

2. Experimental

Multilayer InAs DWELL laser structures have been grown on an Oxford Instruments VG Semicon V90$^+$ MBE system on 3-in n$^+$ GaAs (1 0 0) substrates. The laser design is based on a previously published structure [5] and uses a 1.8 μm $Al_{0.4}Ga_{0.6}As$ waveguide surrounding the active region. The InAs QD–InGaAs QW DWELL structure was grown at ~510 °C and consisted of 2 nm $In_{0.15}Ga_{0.85}As$ followed by 2.9 ML of InAs at a growth rate of 0.09 ML/s and with 6 nm $In_{0.15}Ga_{0.85}As$ layer completing the DWELL. Both thicknesses and compositions were previously optimized as a function of room temperature photoluminescence (PL) intensity. In addition to the laser processing, samples were processed into test mesa diodes and reverse bias measurements were employed as a standard test of device performance.

The morphology of the superficial InAs QDs was investigated using a digital instruments dimension atomic force microscopy (AFM) system in ambient conditions and tapping mode. Cross-sectional transmission electron microscopy (xTEM) specimens were prepared by mechanical polishing followed by ion milling in a Gatan PIPS instrument at low incidence angle and examined in a Philips 420 transmission electron microscope. PL measurements were performed at room temperature with an Ar$^+$ laser emitting at 532 nm and a cooled Ge detector.

3. Results

Multilayer DWELL samples containing three (Vn17) and five (Vn20) repeats and 50 nm barriers were grown using a growth temperature of 510 °C

throughout the active region. All the grown samples exhibited room temperature PL characteristics in the wavelength range 1280–1310 nm. Fig. 1 shows a xTEM micrograph of the three-layer sample, Vn17. This image is free of defects; however, it can be observed that the dot density reduces from $2.3 \times 10^5\,\mathrm{cm}^{-1}$ in the first (lowest) dot plane to $1.7 \times 10^5\,\mathrm{cm}^{-1}$ in the third (highest) one. This reduction of dot density is associated with the presence of defects at low levels. In fact, defects were observed very infrequently in this sample, at a density we estimate in the range 10^{-3}–$10^{-4}\,\mathrm{cm}^{-1}$. Detailed xTEM studies of this structure have shown that QDs are well-confined inside the 8 nm InGaAs QW.

An xTEM image of a five-layer DWELL laser structure (Vn20) is shown in Fig. 2 in which large defected areas are observed. These defected areas are formed from the complex interaction of a number of QDs, nucleating from the first or second dot plane and propagating upwards. Dislocation loops and threading dislocations are generated in these planes, extending to the upper layers. These V-shape defected areas have a density of $\sim 1 \times 10^4\,\mathrm{cm}^{-1}$ and their presence locally reduces the QD density, e.g. the density of dots is reduced from $2.2 \times 10^5\,\mathrm{cm}^{-1}$ to $8.3 \times 10^4\,\mathrm{cm}^{-1}$ from the lowest (first) layer to the uppermost (fifth) layer, Fig. 2b. This reduction comes from indium migration into the dislocated core and produces a distortion in the GaAs barrier regions above these defects. In the low magnification TEM micrograph, Fig. 2b, extended defects in the form of threading dislocations are propagated into the upper cladding regions. The TEM defect characterization has shown that these are formed from a complex entanglement of dislocations and different 60° Burgers vectors are present at the interface. Since the dislocations glide on the (1 1 1) planes and they are only mobile at high temperatures, they must have been formed in the very latter stages of the growth process.

We have found that a modified growth temperature profile has a dramatic effect on the

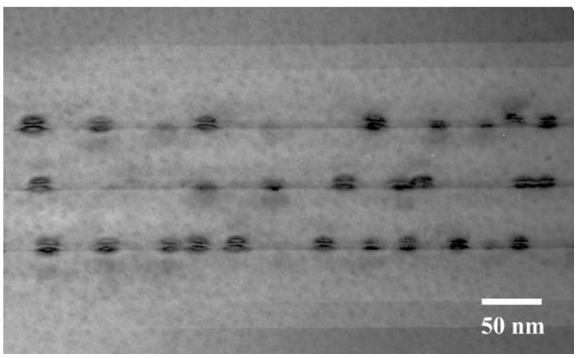

Fig. 1. TEM bright field image of (1 1 0) cross-section image taken under $g = 022$ conditions of the sample Vn17.

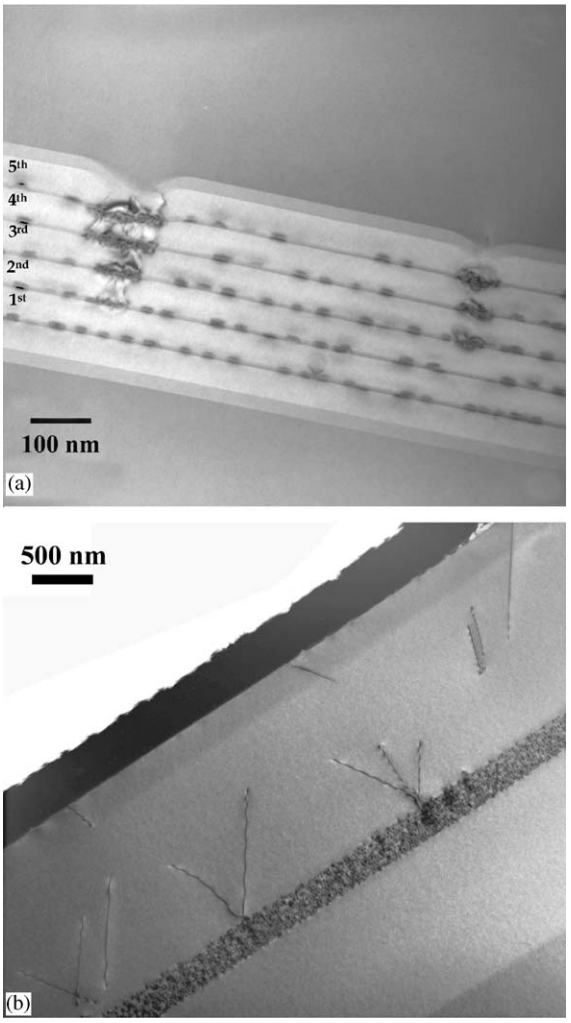

Fig. 2. (1 1 0) Cross-sectional TEM micrographs of sample Vn20 at (a) high magnification using dark field 200 reflection and (b) 220 bright field image at low magnification.

density of dislocations. A micrograph of a five-layer sample (Vn61), which is structurally similar to that of Fig. 2, but in this case the GaAs barrier layer was divided in two parts is shown in Fig. 3. The first 15 nm of the GaAs barrier layers was grown at 510 °C, as before, and the second 35 nm at an elevated temperature of 585 °C. In contrast to the previous sample, the formation of dislocated QDs is completely suppressed by this modified growth method and the QD density is constant through the layers at a value of $1.9 \times 10^5\,\mathrm{cm}^{-1}$.

To investigate the limits of the modified growth method applied to multilayer stacks, we have grown a 10-layer repeat structure with 30 nm GaAs spacer layers (Vn107). Such a multilayer structure is not only for interest in laser structures, but also for detection where an increased absorption is required. This sample exhibits vertical alignment of QDs, in contrast to the samples with a 50 nm spacer (Fig. 4). However, not just QDs, but also the InGaAs barriers show this alignment, with the barrier itself taking on the appearance of a giant QD of dimensions: 265 nm base, 21 nm height and a 15° apex. This effect is remarkable given that no 2D growth mode is normally present for single layers of $In_xGa_{1-x}As$ layer of composition $x = 0.15$ and this illustrates the enhancement of the Stranski–Krastanow (SK) transition due to the underlying strain field. The effect, therefore, is

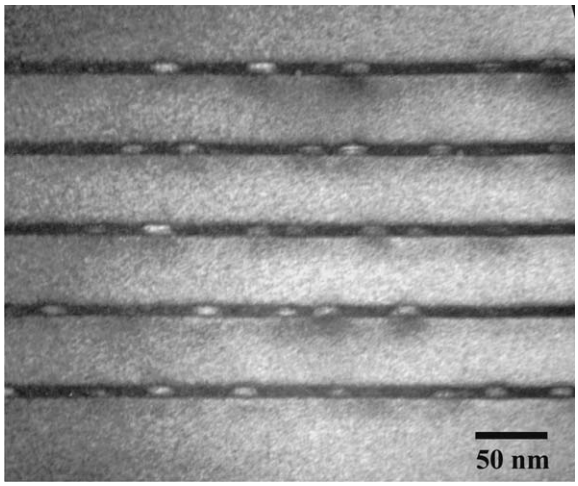

Fig. 3. TEM dark field image of (1 1 0) cross-section image taken under $g = 002$ conditions of the sample Vn61.

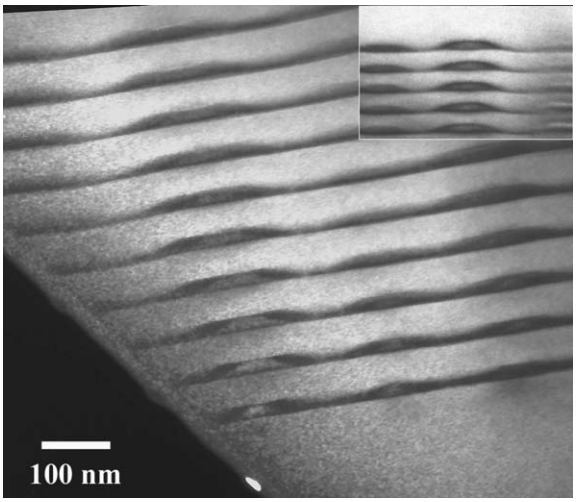

Fig. 4. Dark field ($g = 200$) TEM cross-sectional image of InAs/InGaAs DDOT structure. The insertion shows the TEM cross-section of a stacked $In_{.5}Ga_{.5}As$ QD structure with 12 nm barriers under $g = 002$ dark field conditions.

to create a dot-within-a-dot (DDOT) structure in which the InAs QD sits within a second dot of low indium composition. The inset to Fig. 4 shows a 10-layer stack of $In_{0.5}Ga_{0.5}As$ QDs. This image has remarkable similarities to that of the DDOT sample, showing the similar faceted structure and an indium concentration in the core, which is typical of InGaAs QDs, but with a base of 50 nm width and a height of 12 nm. In this sample, the barrier thickness was 12 nm and we have observed that this is close to the optimum for vertically stacked $In_{0.5}Ga_{0.5}As$ QDs.

4. Electrical and optical characterisation

In Fig. 5 we show the reverse bias electrical characteristics of three- and five-layer samples, both conventionally grown and with the modified high-temperature method. The initial series of samples showed high reverse leakage characteristics, very significantly higher than a test QW sample grown at the same time. The five-layer sample (Vn20) is worse by over one order of magnitude compared to the three-layer sample (Vn17). We have previously attributed reverse leakage in InGaAs multi QW p–i–n diode samples

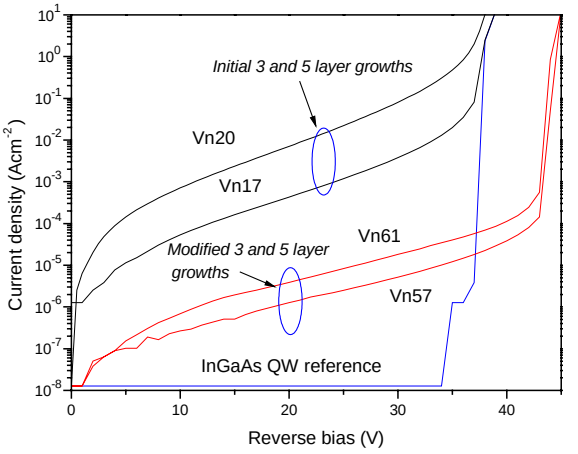

Fig. 5. Reverse bias electrical characteristics of laser samples grown before and after the modification of the growth method. A control laser sample containing pseudomorphic InGaAs QWs is also shown.

to threading dislocation density and believe this to be a sensitive measure of relaxation in such structures [6]. This dependence is also well-known from the studies of silicon-based devices [7] in which it is attributed to the decoration of threading dislocations with metallic precipitates, which act as midgap states, since the dislocations themselves are thought to be electrically neutral. However, in III–V materials this is not necessarily the case as dislocations may be non-stoichiometric and induce mid-gap states without impurities. In either case, the threading dislocation acts as a conducting micropipe [8], traversing the depletion region and emitting and recombining carriers under the high field. Samples grown using the modified growth method, such as Vn61, show reverse leakage characteristics improved by over a factor of two, which we believe is consistent with the reduction in threading dislocation density observed. Using this method, both the three- and the five-layer samples showed excellent lasing characteristics. Room temperature threshold current densities of $\sim$30 A cm^{-1} were observed for the three- and five-layer modified growth method structure, with lasing emission in the range 1294–1302 nm. Both these structures lased under continuous wave conditions at room temperature. In comparison, the three-layer sample using the normal growth method exhibited a five-fold increase in threshold current density, whilst the five-layer heavily defective sample failed to laser under any conditions [9]. The results show that the suppression of threading dislocations is essential for optimal laser operation and that the reverse bias leakage provides a useful characterization method for the presence of defects. It is interesting to note that the leakage values are still not as low as the test QW sample. Due to the finite area sampled, xTEM is insensitive to dislocations below 10^3 cm^{-1}. The presence of threading dislocations therefore cannot be ruled out in the apparently defect-free samples grown using the modified method.

Room temperature photoluminescence (RTPL) characteristics are shown in Fig. 6 for a number of the samples discussed in the structural study. All the samples emit strong RTPL, with a characteristic double peak structure associated with a bimodal distribution of QDs, rather than an excited state transition since the PL excitation power dependence does not change the relative peak intensity. For the case of the modified growth method there is an enhancement of PL intensity of up to a factor of 10 and a reduction in the relative intensity of the lower wavelength peak. This may be explained by the reduction of the density of QDs due to the transfer of material towards

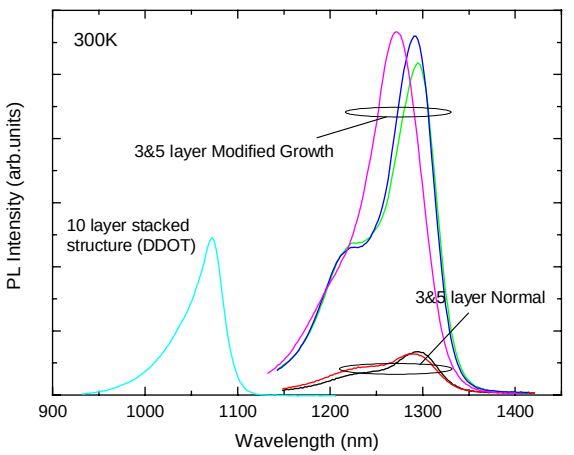

Fig. 6. PL spectra of samples with the normal and modified growth method. The PL of the 10-layer sample, showing the short emission wavelength, is also included.

defective regions. This figure also shows the PL of the ten-layer structure, Vn107. The characteristic 1.3 μm emission wavelength is considerably reduced in this structure to 1.08 μm. At present, we are unable to clarify the reasons for this reduction, however strong indium diffusion out of the QD is expected to be responsible for this effect.

5. Discussion

The origin of the defect mechanism occurring above the second-layer in Fig. 2 is related to defects in the first-layer. By observing the characteristic strain contrast of the samples, in strain sensitive (0 0 4) bright field (BF) xTEM images, we believe that a sizable fraction (~30%) of DWELL QDs are relaxed [10,11], even in single-layer samples. The presence of relaxed QDs can lead to the formation of single or double stacking fault, the latter having a characteristic 'V-shape' as it glides on the {1 1 1} planes towards the surface. We have observed that the glide of these stacking faults to a higher QD layer can nucleates the growth of a large relaxed QD island of volume up to 3–4 times larger than standard dots. Furthermore, we have observed dislocation loop features originating from the coalescence of QDs as a consequence of their high density ($\sim 10^5\,\mathrm{cm}^{-1}$) in these DWELL structures. These two types of defects are habitual in all DWELL samples.

The presence of dislocated QDs considerably distorts the barrier region. This can be understood since relaxed, or dislocated, QDs provide a tensile deformation to the GaAs buffer layer. When the following QD layer is deposited, these depressions act as an effective sink for highly mobile indium adatoms. The preferential formation of InAs islands in this region creates locally very high dot concentrations, which inevitably makes close contact among dots, leading to coalescence and further dislocations. The relaxed region creates a further enhanced depression in the GaAs barrier and the process repeats itself. This chain-effect originates macroscopic V-shape defective regions which themselves can propagate threading dislocations into the barrier. The resulting depression in the GaAs barrier has been observed to reach several 10's of nanometre in depth.

The use of the modified temperature profile, where after 15 nm of capping at low temperature (510 °C) the temperature is increased to 585 °C for the remaining 35 nm, effectively suppresses the formation of these defects. At low temperatures, Ga adatom migration is driven by the strain field and associated with the defective InAs islands. This migration is responsible for the depression in the barrier. However, the strain field will be negligible beyond a certain thickness [12]. At this stage, the non-planar growth front will remain above the dot and the migration of Ga atoms will act to slowly smoothen this strain-free non-planar GaAs surface. The rate of planarization will be increased by increasing the Ga mobility through the growth temperature increase [13]. Therefore, the point at which the transition is made from low to higher growth temperature is quite critical in these structures and our choice of 15 nm for this transition would appear effective. It should be pointed out here that this mechanism is quite distinct from that of Ledentsov and co-workers [14,15], who have reported a technique in which a very thin GaAs cap layer is deposited after the InAs/InGaAs DWELL, followed by a high-temperature (>600 °C) selective evaporation of uncovered larger dislocated dots. This mechanism is unlikely to operate in the present structures that use a much thicker cap (15 nm) and a lower temperature (585 °C). In addition there is no evidence for large unfilled voids in the TEM images that might be expected from the method they discuss.

In the case of the 10-layer structure, where the spacer thickness was reduced from 50 nm to 30 nm, lateral ordering in the structure was induced, instead of the random location of the previous structures. The high strain field orders both the well and the dot. The change of the InGaAs well to a faceted dot structure shows the influence of the underlying strain field on the growth mode, since a composition of 15% is not expected to undergo the SK transition. A close observation of this figure shows that the well modulation builds up in the first and second-layers, as the strain progressively increases. The stacking behaviour we observe is

very similar to that seen in $In_{0.5}Ga_{0.5}As$ QDs with an optimum barrier thickness of 12 nm. The effective stacking with 30 nm barrier thickness and the larger size is concurrent with the view that the system can be scaled as a function of the strain. The resulting structure we term as a 'dot-in-dot' (DDOT) structure. At present, we are not able to clarify the compositional profile of this novel structure. The short wavelength indicates that considerable out diffusion of indium may have taken place from the dot to the well. This work will be the subject of further studies to determine the composition profile of this novel structure.

6. Conclusions

We have observed that relaxation of InAs QDs based on the DWELL structure is a significant phenomenon and that its effect on subsequent layers must be considered in multilayer samples with finite spacer thicknesses. In addition, for the DWELL samples we have used with 2 nm InGaAs below the QD, a significantly higher dot density is observed which is highly desirable for efficient optical emission. However, due to the high island density, coalescence of QDs occurs, acting as a further mechanism for the generation of dislocations that can propagate upwards.

In multilayer samples, dislocations, which nucleate around incoherent islands or from island coalescence, may extend through subsequent dot layers. The interaction of these dislocations with the subsequent layers is observed to produce a local tensile deformation of the GaAs barrier, encouraging Ga migration away from the relaxed region and In migration towards the relaxed region. The local increase in indium concentration nucleates clusters of QDs. The overall effect is to create defected regions composed of clusters of dislocated dots propagating threading dislocations into the cladding regions that severely degrade the optical and electronic quality of laser structures. The effects are seen in PL and are especially sensitive in reverse bias diode leakage measurements. The use of the modified high-temperature growth method improves the planarity of the GaAs buffer and effectively prevents the propagation of this disturbance to the subsequent dot planes. As a result, improved PL and electrical characteristics are observed. Processed laser devices with these samples exhibit room temperature threshold currents $\sim 30\,A\,cm^{-1}$, amongst the best reported in the literature.

Acknowledgements

This work is supported by the UK EPSRC, and the European Commission Framework 5 project 'NANOMAT'. One of us (M.G.) acknowledges the support of the Ministerio de Educación Cultura y Deporte of the Government of Spain.

References

[1] X. Huang, A. Stinz, C.P. Hains, G.T. Liu, J. Cheng, K.J. Malloy, Electron. Lett. 36 (2000) 41.
[2] G. Park, O.B. Shcheekin, S. Csutak, D.L. Huffaker, D.G. Deppe, Appl. Phys. Lett. 75 (1999) 3267.
[3] G.T. Liu, A. Stintz, H. Li, K.J. Malloy, L.F. Lester, Electron. Lett. 35 (1999) 1163.
[4] A.E. Zhukov, A.R. Kovsh, N.A. Maleev, S.S. Mikhrin, V.M. Ustinov, A.F. Tsatulnikov, M.V. Maximov, B.V. Volovik, D.A. Bedarev, Yu.M. Shernyakov, P.S. Kopev, Zh.I. Alferov, N.N. Ledensov, D. Bimberg, Appl. Phys. Lett. 75 (1999) 13.
[5] H.Y. Liu, M. Hopkinson, C.N. Harrison, M.J. Steer, R. Frith, I.R. Sellers, D.J. Mowbray, M.S. Skolnick, J. Appl. Phys. 93 (2003) 2931.
[6] J.P.R. David, Y.H. Chen, R. Grey, G. Hill, P.N. Robson, P. Kightley, Appl. Phys. Lett. 67 (1995) 906.
[7] M.V. Whelan, Solid-State Electron. 12 (1969) 963.
[8] V.I. Talanin, I.E. Talanin, D.I. Levinson, Cryst. Res. Technol. 37 (2002) 983.
[9] H.Y. Liu, I.R. Sellers, M. Gutierrez, K.M. Groom, W.M. Soong, M. Hopkinson, J.P.R. David, R. Beanland, T.J. Badcock, D.J. Mowbray, M.S. Skolnick, J. Appl. Phys. 96 (2004) 1988.
[10] F. Ernst, P. Pirouz, J. Mater. Res. 4 (1989) 834.
[11] H.L. Tsai, R.J. Matyi, Appl. Phys. Lett. 55 (1989) 265.
[12] G. Biasiol, E. Kapon, Phys. Rev. Lett. 81 (1998) 2962.
[13] H. Saito, K. Nishi, S. Sugou, Appl. Phys. Lett. 74 (1999) 1224.
[14] N.N. Ledentsov, US Patent Number 6,653,166 B 2 Nov. 25, 2003.
[15] D.S. Sizov, M.V. Maksimov, A.F. Tsatsul'nikov, N.A. Cherdashin, N.V. Kryzhanovskaya, A.B. Zhukov, N.A. Maleev, S.S. Mikhrin, A.P. Vasil'ev, R. Selin, V.M. Ustinov, N.N. Ledentsov, D. Bimberg, Z.I. Alferov, Semicon. 36 (2002) 1020.